An experimental study of process parameters in the manufacture of Ti-6Al-4V and Cr-Co spherical prostheses

J.V. Abellán-Nebot – H. R. Siller – C. Vila – C.A. Rodríguez

J. V. Abellán-Nebot – C. Vila

Department of Industrial Systems Engineering and Design. Universitat Jaume I. 12071 Castellón. Spain.

H. R. Siller* – C. A. Rodríguez

Centre for Innovation in Design and Technology. Instituto Tecnológico de Estudios Superiores de Monterrey. Monterrey 64700, México.

Tel. (52) 8183582000 ext. 5149

Fax. (52) 8183581209

*e-mail: hector.siller@itesm.mx

Abstract

Ti-6Al-4V and *Cr-Co* alloys are extensively used in manufacturing prostheses due to their biocompatibility, high strength-to-weight ratio and high resistance to corrosion and wear. However, machining operations involving *Ti-6Al-4V* and *Cr-Co* alloys run up against a series of difficulties related with their low machinability which complicate the process of controlling the high quality (surface roughness and form tolerances) required in these parts. The major concern of this paper is to study the effects of process variables (cutting parameters, machine-tool and CNC variables, and parameters related to the inspection in a coordinate measurement machine) and geometric features on surface roughness parameters and form errors in *Ti-6Al-4V* and *Cr-Co* alloys test pieces. The machining performance of the two biocompatible materials is compared, focusing on part quality at low feed rates and the stochastic nature of plastic deformations in this regime. In addition, a multi-sensor system based on accelerometers and an acoustic emission sensor was mounted to investigate whether these low-cost non-intrusive sensors could be used to obtain more reliable predictions about machining performance in terms of surface roughness and spherical form deviation using linear regressions.

Nomenclature	Description
A	Nose angle
AE	Acoustic Emission Sensor
CNC	Computerized Numerical Control
CMM	Coordinate Measuring Machine
Cr-Co	Chromium Cobalt alloy
d	Depth of cut
DoE	Design of Experiments
f	Feed rate
r	Nose radius
R	Spherical features Radius
R_a	Arithmetical mean roughness
R_y	Maximum peak roughness depth
R_z	Ten-point mean roughness depth
R_{zt}	Theoretical Ten-point mean roughness depth
RMS AE	Root Mean Square of AE signal
RMS Accel x	Root Mean Square of Accelerometer Signal X direction
RMS Accel y	Root Mean Square of Accelerometer Signal Y direction
RMS Accel z	Root Mean Square of Accelerometer Signal Z direction
Ti-Al_V	Titanium aluminium Vanadium alloy
V_B	Tool flank wear
v_c	Cutting speed

1. Introduction

Recent efforts to find biocompatible materials for human bone replacement have turned towards the synthesis of new metallic and polymeric materials and, therefore, the emergence of enhanced manufacturing processes. The results of these developments have improved the life expectancy and the comfort of patients with bone diseases and damages. Moreover, cases of rejection of orthopaedic implants (prostheses) have decreased due to the biocompatibility achieved with the use of ultra-high molecular weight polyethylene (UHMWPE), *Cr-Co* alloys, titanium alloys (mostly *Ti-6Al-4V*) and other state-of-the-art metals, polymers and ceramics.

Ti-6Al-4V and *Cr-Co* alloys have been used due to their good behaviour in terms of toughness, strength, low thermal conductivity and resistance to corrosion. The former possess enhanced biocompatibility, higher strength-to-weight ratio, reduced elastic modulus and superior resistance to strain-controlled and notch fatigue. In comparison, *Cr-Co* alloys are more resistant to corrosion and wear, and are more suitable for certain kinds of prostheses that are in contact with highly corrosive environments [1]. Furthermore, in total joint replacement, wear rates of femoral heads made of *Ti-6Al-4V* have been reported to be 35% greater than those of *Cr-Co* in hip simulator testing [2].

Manufacturing processes for metallic prostheses involve several forming operations (casting, forging or sintering), machining operations (conventional and alternative), and finishing processes (hand and mechanical polishing) (Figure 1).

The challenge of finding appropriate combinations of quality, productivity and costs has led different research groups to explore and understand processing behaviour through exhaustive experimentation, process modelling and simulation. Because titanium alloys are also being used to manufacture aerospace components, research work in the field of machining operations is widespread [3-9]. In these works, the authors conducted comprehensive studies on tool life, cooling techniques, chip formation mechanisms and other factors that influence the machinability of these alloys. However, very few studies deal with the machinability of *Cr-Co* alloys used in surgical and orthopaedic devices [10, 11]. Furthermore, no comparative studies (in terms of the machinability of the two biocompatible materials) have been published previously.

Prostheses Manufacturing demands different quality parameters than those demanded by aerospace applications. For example, it is necessary to ensure that highly polished surface finishes or specialised textures are achieved in order to avoid releasing wear debris or to promote healthy tissue-biomaterial interactions, respectively [12]. Otherwise, adverse effects such as cellular damage, infections, blood clots and failure of the implants can appear [13].

Fig. 1 Manufacturing route for metallic components of prostheses.
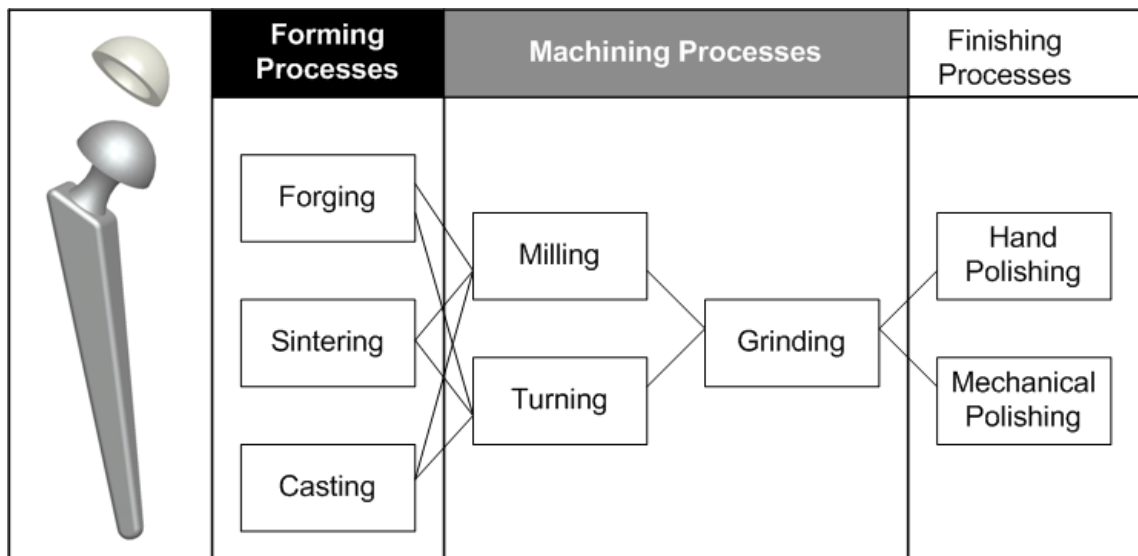
[Insert Figure 1]

In general, most prosthetic joints, like femoral heads, acetabular cups and knee replacements, require a high surface quality and tight form tolerances. These requirements force manufacturers to follow a process plan consisting of three consecutive material removal processes: turning or milling, grinding and polishing. Machining operations involving *Ti-6Al-4V* and *Cr-Co* alloys face a series of difficulties related with low machinability, including:

a)   Very high temperatures at the tool-workpiece interface;

b)   Localised plastic instability; and

c)   Excessive tool wear caused by diffusion and chemical reactivity [14].

These factors make difficult to keep surface roughness and form tolerances under control, which results in higher processing times and costs during the grinding and polishing steps. In addition, the capability to keep parts within tight form tolerances is severely limited in grinding operations because of the thermal deformations that occur during metal removal. The present study focuses on machining operations in the manufacture of prostheses, with special attention being paid to spherical turned components in hip prostheses. The purpose of the procedure outlined in this paper is to determine the most critical process variables related to surface roughness and spherical form deviations (ε) through minimal Design of Experiments (DoE). In order to study the resultant surface geometry, three different surface roughness parameters are analysed: *Ra*, *Ry*, and *Rz*. These three parameters must be analysed simultaneously for controlling the surface roughness profile accurately [15]. For example, peaks and valleys on the surface should be controlled, since they may result in the generation of friction and heat between moving parts and corrosion of the surface over a long service period [16]. In the study, the influence of machine-tool, CNC variables and cutting parameters on part quality are analysed and discussed in detail. Furthermore, the influence of CMM parameters on the inspection of the sphericity of the parts are also analysed and discussed. In addition, the study analyses the different measurements acquired by a low-cost non-intrusive multi-sensor system in order to evaluate whether its use in this specific application can improve the prediction of machining performance in order to control the cutting operation.

2. Manufacturing and inspection process parameters.

The high quality required (surface roughness and form tolerances) in the manufacturing of spherical prostheses makes necessary a thoroughly analysis of the process variables distinguished as relevant in the manufacturing and inspection process:

I. Machine-tool and CNC errors due to their influence on the cutting-tool path deviation from nominal values;

II. Cutting parameters due to their relationship on how the material is removed; and

III. CMM parameters due to their relationship on how the part is inspected and the resulting measuring uncertainty.

2.1 Machine-tool and CNC errors

During turning operations demanding tight tolerances, machine tool dynamics and control accuracy are important sources of error. Machine-tool errors include geometric and thermal errors. Geometric errors are those errors that are extant in a machine on account of its basic design and the inaccuracies built-in during the assembly of machine-tool components [17]. Thermal errors are those that cause a relative displacement between the workpiece and the tool on account of deformation or expansion of the machine elements due to an increase in their temperature [18]. These errors are difficult to be evaluated and require costly equipment such as ball bars or interferometer systems. On the other hand, errors related to the CNC include chordal errors, tracking errors and contour errors.

Chordal errors are characteristic of linear interpolations in CNC programs, and are due to the discretization of the desired tool path in small linear interpolations, which are followed by the tool in the actual machining operation. Maximising the number of segments as much as possible, leads to reduce the deviation of the cutting-tool trajectory from the nominal profile and to increase the curve smoothness. Furthermore, a trajectory that presents a discontinuity of segmentation can lead to a deterioration of the surface accuracy [19]. However, when the trajectory is composed of too small segments, the tool never reaches the desired speed, due to the acceleration/deceleration phases automatically applied at the beginning and end of each segment by the position control servomechanisms. As a result, the feed is not constant throughout the curve, which can lead to poor surface finish [20].

The trajectory defined in the CNC codes should be followed and controlled by the servomechanisms. For this purpose, the axis controller in a machine-tool provides the appropriate drive signals to the motors so that the actual position of the axis precisely 'tracks' the required axis reference command provided by the CNC, with the aim of eliminating any position error for each driving axis. However, due to the unbalance degree of the gains of the control systems for the axes, friction in the guideways, etc., a positioning error in each machine-tool axis is presented, which is called the tracking or following error [20]. If the positioning error is evaluated on the contour, and not on each machine-tool axis, the positioning error is called contour error, which is defined as the actual difference in distance between the programmed cutting-tool trajectory and the actual trajectory [21].

Some CNC parameters such as the look-ahead parameter can be used in order to keep the real trajectory closer to the ideal one and improve dimensional part quality. Through this parameter, the control adjusts the feed speed to give the servos sufficient time to accelerate or decelerate minimising the contour error. The machine-tool can then make straight line motions, track corners or make broad curves at the highest feed speed value requested, whereas the feed speed is automatically reduced when the curvature of the trajectory requires it [20].

2.2. Cutting parameters

Cutting parameters such as cutting speed, feed rate or depth of cut among others should be defined by process planners to achieve part quality specifications at minimum cost. It is well-known that the cutting speed influences on the formation of built-up edge which produces a higher surface roughness; the feed rate directly influences on the surface roughness due to the cutting-tool marks during the material removal; and the depth of cut influences on the cutting forces required for material removal and thus, on the part deflection during turning. The literature that documents these effects is extensive [22-24], but in the case of prostheses manufacturing with strict surface roughness specifications the knowledge is still incipient.

2.3 CMM parameters

Nowadays, most of the CMM present mathematical compensation algorithms that allow keeping geometric and thermal errors below 3 μm [29]. Other source of errors are related to the jigs and fixturing mechanisms which affect the datum information, although these sources are negligible if the part quality measurement is related to an intrinsic characteristic such as roundness, sphericity or run-out [30]. Apart from these sources of errors, the measuring strategy has a special importance to assure part specifications, since it can define most of the measurement uncertainty, especially when measuring an intrinsic characteristic of a feature.

3. Experimental Procedure.

The experimental setup applied in the study is shown in Figure 2 and it is summarised in Table 1. In the experimentation, the faces of two cylindrical bars of *Ti-6Al-4V* and *Cr-Co* alloys were contoured for each parameter combination. As shown in Figure 3, two operations were conducted: a roughing operation to shape the parts, and a finishing operation to give the parts a spherical shape with the required geometrical specifications. For finishing operations, the ranges of cutting parameters recommended by the cutting-tool catalogues are the following:

  i) for *Ti-6Al-4V* alloys, cutting speed, V_c (m/min) ∈ [40,80]; feed rate, f_n (mm/min) ∈ [0.05,0.2]; step depth, a_p (mm) ∈ [0.1,0.3];

  ii) for *Cr-Co* alloys, V_c (m/min) ∈ [15,35]; f_n (mm/min) ∈ [0.05,0.15]; a_p (mm) ∈ [0.1,0.3].

 The spherical features analysed in the experimentation are geometries commonly presented in the manufacture of femoral prostheses, where the radius of the spherical feature *R* measures 10 to 30 mm depending on the patient size. The finishing operations were always conducted using new cutting inserts in order to avoid the impact of cutting-tool wear on surface roughness.

The lathe used for the experimentation was a Lealde TCN-10 with a CNC Fagor 8055. After machining, detailed measurements of *Ra*, *Ry*, *Rz* and *ε* were conducted through a profilometer and a coordinate measuring machine (CMM). Some specifications of these measurement instruments can be found in Table 2. The measurement of *Ra*, *Ry* and *Rz* was obtained as the average of three measurements in three different zones of the

spherical surface, whereas the measurement of ε was obtained after measuring 9 points on the spherical feature with the CMM, as shown in Figure 4.

Table 1. Experimental setup

WORKPIECES		
Ti-6Al-4V Alloy	*Denomination*	ASTM B348-05
	Composition by weight %	Al 6.31, V 4.09, Fe 0.13, C 0.15, N 0.007, O 0.13, Ti Remainder
Cr-Co Alloy	*Denomination*	ASTM F1537-00
	Composition by weight %	C 0.052, Si 0.34, Mn 0.54, P 0.004, S 0.004, Cr 27.36, Mo 5.62, Ni 0.18, Co 65.15
Geometry		Bars with 60 mm dia.
CUTTING TOOL		
ISO Denomination		SRDCN2020K10
Insert ISO Denomination		RCMT 0502M0
Insert Dimensions		Round d = 5 mm (r_e = 2.5 mm)
Edge Preparation rake angle		$\gamma = 15°$
Clearance angle		$\alpha = 7°$
Insert material		Tungsten carbide (WC) without coating
MACHINE TOOL		
Model		Lealde TCN-10
Axis Accuracy		X- axis: ±3 μm
		Z- axis: ±7 μm

[Insert Table 1]

Table 2. Measurement equipment for experimental work

| SURFACE ROUGHNESS	
Profilometer	MITUTOYO SURFTEST 301
Measure Repeatability	0.02 μm
Sampling length and number of spans (n)	λ_c/L = 0.25 mm, n = 1 (if R = 10 mm) n = 3 (if R = 30 mm)
3D MEASUREMENT	
Coordinate Measuring Machine (CMM)	Brown & Sharpe Mistral 10.07.05
Touch Trigger probe	TP2
Touch probe	A-5000-7806
Probe ball diameter	1 mm
Measure Repeatability	1 μm
Measurement resolution	0.2 μm

[Insert Table 2]

Fig. 2 Experimental setup
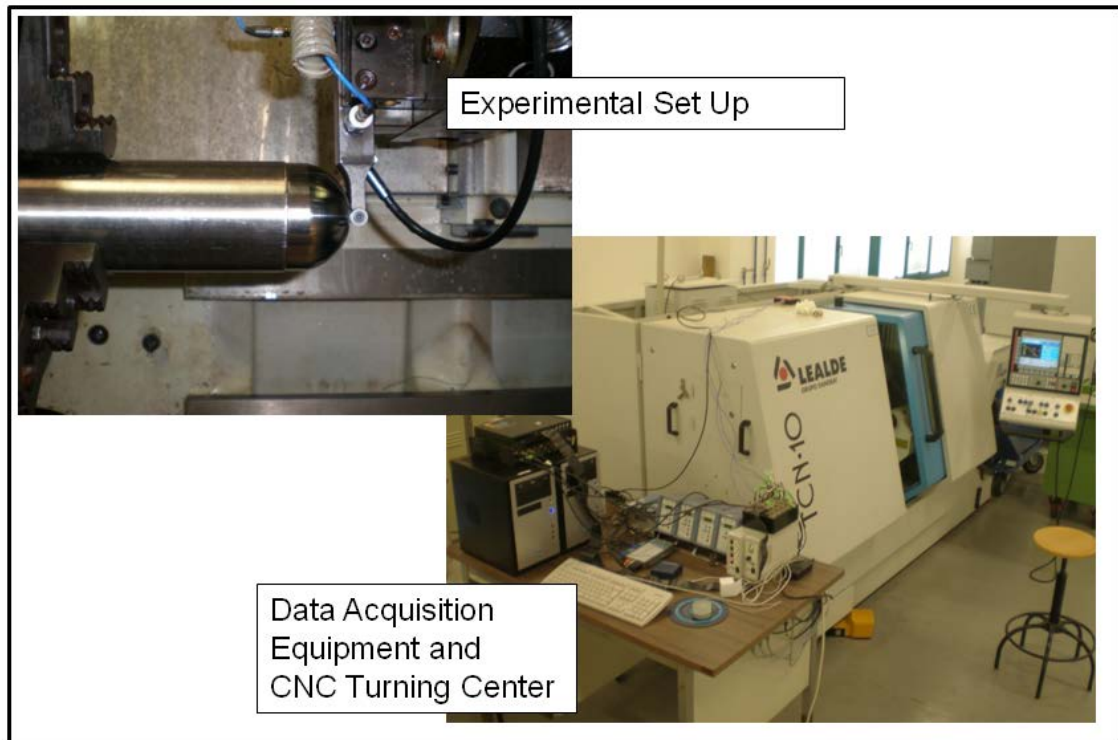
[Insert Figure 2]

In order to monitoring the cutting operation, a multi-sensor system composed of three accelerometers in the X, Y, Z directions and one acoustic emission sensor was installed on the cutting-tool holder. This multi-sensor system was based on low-cost non-intrusive sensors, suitable for both dry and wet machining conditions. All sensor signals were first conditioned and filtered to acquire only the data within the range of interest. The Root Mean Square (RMS) value of each accelerometer was evaluated during each cutting operation and the RMS of the acoustic emission signal was read directly from the sensor output. Figures 3 and Figure 4 show the data acquisition equipment and the location of the sensors in the cutting-tool holder respectively. Table 3 shows the sensor specifications used in the experimentation.

Fig. 3 Machining operations carried out in the experimentation
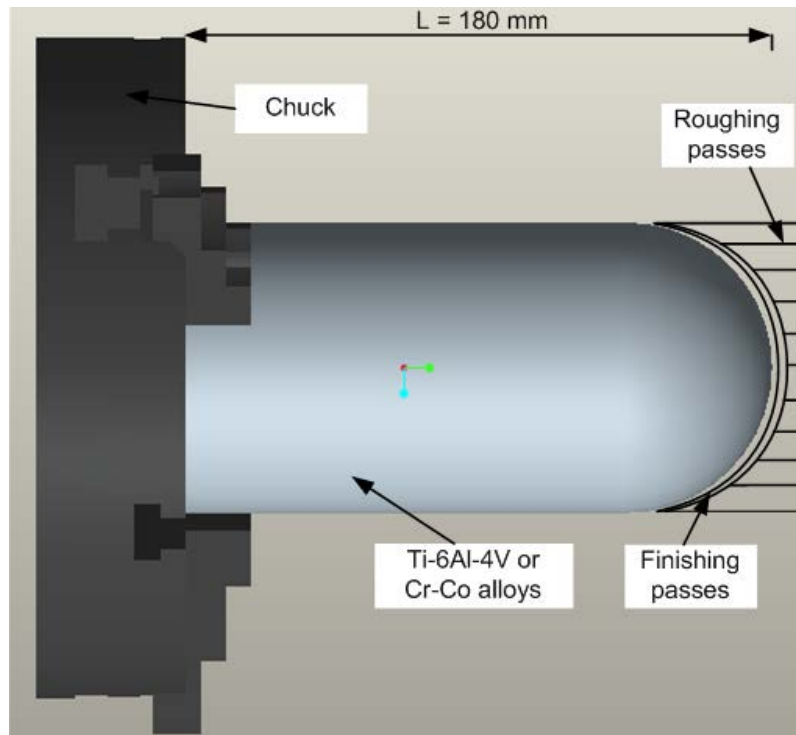
[Insert Figure 3]

Fig. 4 Equipment and Setup for off-line and in-process measurements
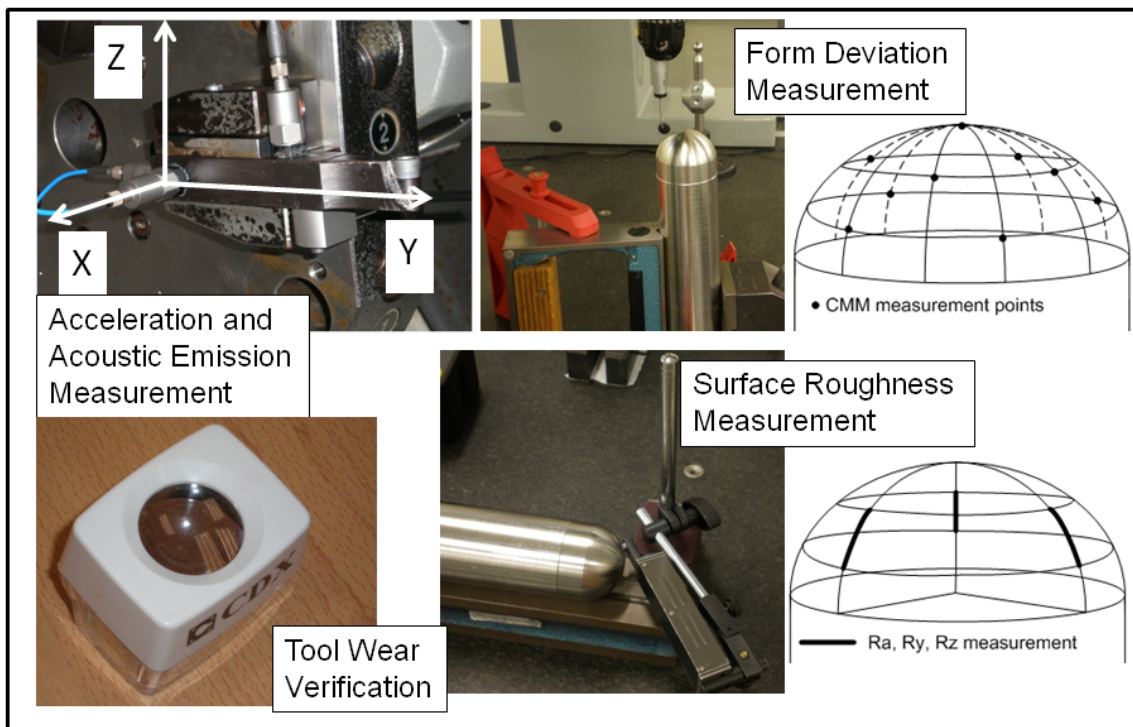
[Insert Figure 4]

Table 3. Sensors used in the experimentation

Accelerometers	
Type	PCB 353B04
Sensitivity	10 mV/g
Signal condition	PCB 482A22 (Gain 10)
Digital Filter	5th order Butterworth Lowpass filter (Fc = 2 kHz)
Sample frequency	50 kHz
Axis measurement	X, Y, Z
Location	Toolholder
Acoustic Emission	
Type	Piezotron 8152B118
Sensitivity	57 dBref 1V/(m/s)
Signal condition	Piezotron coupler 5125B (Gain 10)
Analogue Filter	Built-in Butterworth High-pass filter (Fc = 50 kHz) 40dB
Sample frequency	50 kHz
Location	Toolholder

[Insert Table 3]

4. Study of the influence of CNC errors.

The case study presented in this paper shows the manufacturing process of spherical features of femoral prostheses. These features are directly programmed in the CNC by circular interpolation commands in ISO codes and manufactured in a single phase. The geometric feature was extracted of parts from prostheses with a spherical component with radius between 10-30 mm, and the critical form error to be kept under control is their sphericity, which is an intrinsic characteristic of the feature and it is independent to any datum.

For this application, chordal errors do not apply since there is no post-processed code from CAD/CAM software. Furthermore, geometric errors which can be important when machining large parts can be considered negligible due to the small size of the features

machined. Similarly, thermal errors which are important when the machining time for one part is large or when extrinsic tolerances should be controlled, can be also considered negligible. Thus, it can be assumed that the most important error from those explained above is the following error or contour error, whose effects will be analysed through a DoE.
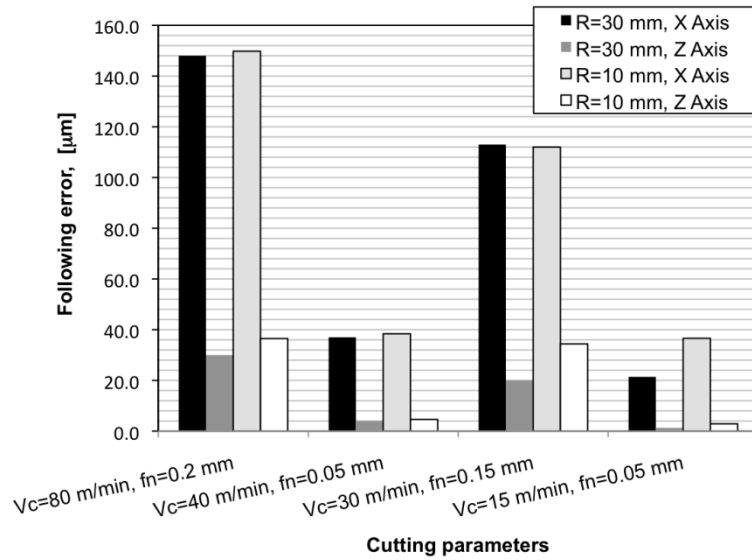
4.1 Design of Experiments.

As shown in Table 1, according to vendor specifications the dynamic accuracy of the CNC lathe in X and Z axis is ± 3 μm and ± 7 μm respectively, which limits the achievable accuracy of the spherical features to this range. In order to quantify the deviation of the cutting-tool trajectory for the manufacture of spherical prostheses, a short DoE is conducted. Due to the nature of the contour error, the expected influent factors are the feed speed and the radius of the tool path which defines the smoothness of the trajectory. The measurement of the contour error will be obtained by saving in internal variables of the PLC of the machine-tool, the actual position of the X and Z axis defined by the encoders signals and the desired X and Z positions. The number of points analysed were 6 equidistant points in the circular trajectory. Additionally, the following errors of each axis stored in internal variables of the PLC were also saved. Therefore, the DoE considers the cutting combinations for both materials that define the fastest and the lowest feed movements of the tool for both size of spherical features (radius of 10 and 30 mm).

4.2 Analysis and discussion of the experimental results.

The results of this DoE are shown in Figure 5 and Figure 6. The first Figure shows the maximum following error of each axis at each cutting combination and curvature of the trajectory. As it can be seen, when the cutting conditions define higher feeds of the tool, such as $V_c = 80$ m/min and $f_n = 0.2$ mm or $V_c = 30$ m/min and $f_n = 0.15$ mm, the following error increases which could lead to contour errors. Furthermore, for the same cutting conditions, following errors are slightly higher for cutting trajectories with a lower radius of curvature since these trajectories are less smooth. However, in spite of the high values of the following errors reported, the contour errors generated in the part keep a tight tolerance on the sphericity of the part as shown in Figure 6. In this Figure it can be seen that, due to the imperfection of the machine-tool, the sphericity error of the parts is lower than 9 μm for any of the cutting conditions tested. It can be noted that the higher sphericity errors are related to those cutting conditions with higher feeds, and thus, with higher

following errors. Furthermore, the higher sphericity errors are presented when conducting trajectories with a lower radius of curvature since the changes on the tool movements are less smooth.

Fig. 5 Following errors of X and Z axis for different cutting combinations and radius of curvature.

[Insert Figure 5]

Fig. 6 Sphericity error of the cutting-tool trajectory for different cutting combinations and radius of curvature.

[Insert Figure 6]

13
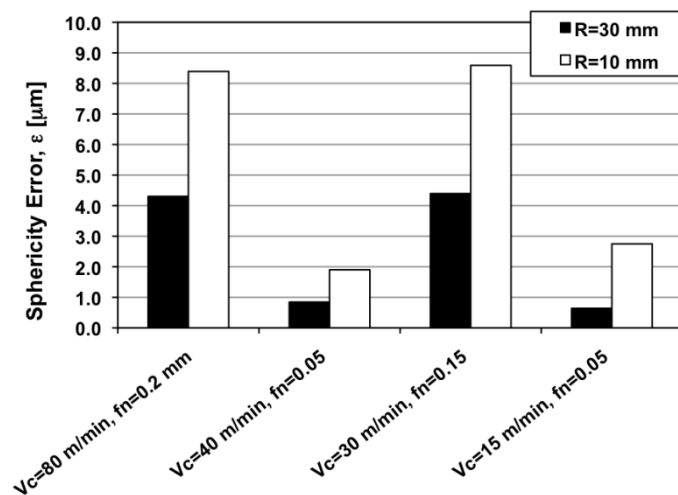
5. Study of the influence of cutting parameters.

5.1 Design of Experiments.

In order to study the cutting process of the joint prostheses analysed in this work with the minimum amount of experimentation, an additional fractional factorial DoE with resolution IV was conducted. In this DoE, four two-level factors were defined for the two prosthesis materials that were analysed, namely: cutting speed (V_c); feed rate (f_n); step depth (a_p); and radius of the spherical feature (R). Through this DoE (resolution IV), the main effects are confounded with the three-factor interactions, which can be assumed to be negligible, and the two-factor interactions that were analysed were those including only cutting parameters, since they are related to chip formation. Table 4 shows the two-level factors analysed in the DoE, selected following the cutting-tool catalogue recommendations for finishing operations, and the DoE aliasing structure. Two replicates were conducted in a random order to obtain information about surface roughness parameters (Ra, Ry, and Rz) and spherical form deviation (ε) at each experimental setting. Tables 5 and 6 show the experiments that were conducted and the resulting measurements of Ra, Ry, Rz and ε for both biocompatible materials.

Table 4. Factors and levels analysed in the Design of Experiments

	Cutting Speed V_c (m/min)	Feed rate f_n (mm/rev)	Step depth a_p (mm)	Radius Feature R (mm)
Ti-6Al-4V Alloys	40-80	0.05-0.2	0.1-0.3	10-30
Cr-Co Alloys	15-35	0.05-0.15	0.1-0.3	10-30
DoE Aliasing structure:	$V_c \, x \, f_n = ap \, x \, R; \; V_c \, x \, a_p = f_n \, x \, R; \; V_c \, x \, R = f_n \, x \, a_p$			

[Insert Table 4]

Table 5. Design of Experiments that was conducted and the resulting measurements of surface roughness and form deviation. Workpiece material: *Ti-6Al-4V* alloys

V_c (m/min)	f_n (mm/rev)	a_p (mm)	R (mm)	Ra (µm)	Rz (µm)	Ry (µm)	ε (µm)	Accel. RMS X (mV)	Accel. RMS Y (mV)	Accel. RMS Z (mV)	AE RMS (mV)
80.00	0.05	0.10	30	0.20	0.90	1.50	3.0	108.7	108.3	95.7	1285
40.00	0.05	0.30	30	0.21	1.13	1.43	5.2	154.9	75.1	77.1	1054
40.00	0.05	0.30	30	0.20	1.07	1.63	6.0	152	85.3	68.3	800
80.00	0.20	0.30	30	0.41	2.07	2.60	5.2	579	186	180	4606
40.00	0.20	0.10	30	0.35	1.63	2.13	5.5	183	102.7	76.7	1198
40.00	0.20	0.10	30	0.44	1.77	2.43	5.7	188.6	97	82	1783
80.00	0.20	0.30	30	0.51	1.90	2.60	5.3	706	285	126	5306
80.00	0.05	0.10	30	0.19	1.00	1.70	4.6	252.7	148.5	107.2	1267
40.00	0.05	0.10	10	0.27	1.43	1.43	5.7	130.2	112.6	93.9	1263
40.00	0.20	0.30	10	0.30	1.57	1.57	7.8	538	327	230	6047
80.00	0.05	0.30	10	0.25	1.23	1.23	6.0	181	149	121.7	2091
40.00	0.20	0.30	10	0.30	1.43	1.43	3.0	435	296	215	5765
80.00	0.05	0.30	10	0.25	1.30	1.30	6.9	82.4	93.56	81.57	859
80.00	0.20	0.10	10	0.33	1.70	2.17	5.3	232	241.8	181.2	3348
80.00	0.20	0.10	10	0.32	1.60	1.60	3.0	271	141.6	113	1972
40.00	0.05	0.10	10	0.23	1.30	1.30	4.0	120.2	114.2	97	1621

[Insert Table 5]

Table 6. Design of Experiments that was conducted and the resulting measurements of surface roughness and form deviation. Workpiece material: *Cr-Co* alloys

V$_c$ (m/min)	f$_n$ (mm/rev)	a$_p$ (mm)	R (mm)	Ra (µm)	Rz (µm)	Ry (µm)	ε (µm)	Accel. RMS X (mV)	Accel. RMS Y (mV)	Accel. RMS Z (mV)	AE RMS (mV)
35.00	0.05	0.10	30	0.30	1.67	2.13	2.8	166.4	82.2	69.6	1322
15.00	0.05	0.30	30	0.33	1.67	2.23	4.3	344	171	180	1540
15.00	0.05	0.30	30	0.35	1.70	2.23	5.1	274.8	204.3	130.9	1344
35.00	0.15	0.30	30	0.34	1.67	2.03	9.9	704	672	378	9992
15.00	0.15	0.10	30	0.35	1.73	2.20	4.5	727.8	244.6	573.8	1187
15.00	0.15	0.10	30	0.34	1.57	1.83	4.2	690	271	319	1028
35.00	0.15	0.30	30	0.30	1.67	2.03	6.4	913	489	219	9976
35.00	0.05	0.10	30	0.29	1.53	2.00	5.5	172.8	84.5	71.5	1350
15.00	0.05	0.10	10	0.25	0.97	0.97	6.0	191	125	59.7	2354
15.00	0.15	0.30	10	0.37	1.70	1.70	3.9	758	235	262	1314
35.00	0.05	0.30	10	0.29	1.17	1.17	7.0	714	150	57.8	2701
15.00	0.15	0.30	10	0.38	1.80	1.80	4.2	712	221	423	1329
35.00	0.05	0.30	10	0.27	1.13	1.13	4.7	716	140	75.6	2517
35.00	0.15	0.10	10	0.34	1.93	1.93	8.2	519	178	84	5516
35.00	0.15	0.10	10	0.36	1.73	1.73	3.6	463	139	77	3370
15.00	0.05	0.10	10	0.34	2.33	2.33	5.0	163	82.3	66	1515

[Insert Table 6]

5.2 Analysis and discussion of the experimental results.

A Pareto chart of standardised effects was plotted for each performance variable in order to assess the significance of the main effects and interactions analysed in each prosthesis material that was studied. The results, summarised in Table 7, show the importance of f_n and the interaction $V_c x a_p$ for *Ra, Ry* and *Rz* when turning *Ti-6Al-4V* alloys. Additionally, the interaction $V_c x f_n$ is also important for *Rz*, whereas the factor *R* is important for *Ry*. The obvious importance of f_n in surface roughness parameters is explained by the cutting-tool marks that are left when material removal occurs, even at low feed rates when plastic deformation effects appear. Other significant interactions such as $V_c x a_p$ and $V_c x f_n$ could be explained due to their influence on cutting vibrations and chip formation respectively. The influence of *R* on *Ry* occurs because the surface length analysed when R is low should be smaller (number of spans equal to 1 instead of 3), since the profilometer cannot deal with surfaces with high curvatures. Thus, on analysing a smaller length, the highest peak

16

and valley measured by the *Ry* parameter tend to be lower than when a larger length is analysed. Factor *R* has no influence on *Ra* and *Rz*, its influence on *Ry* is due to the limitations of the profilometer when measuring surfaces with high curvatures.

Unlike *Ti-6Al-4V* alloys, *Cr-Co* alloys present a highly random behaviour as regards surface roughness parameters and only the feed rate is slightly significant for the *Ra* parameter. The *Rz* parameter presents a high degree of variability that prevents any significant cutting parameter or interaction from being defined. The *Ry* parameter also presents the factor *R* as significant, which can again be explained in a similar way to the reasoning conducted above. The low correlation between any surface roughness parameter and the main effects or interactions is an important issue to be considered when tight surface roughness specifications are required in the turning of *Cr-Co* alloys.

With regard to spherical form deviations, Table 7 shows that any main effect or interaction is significant for both *Ti-6Al-4V* and *Cr-Co* alloys. In fact, the low form deviation that is measured, which is below 10 *μm* in any cutting parameter combination, could be mostly explained by the accuracy of the CNC lathe (as shown in section 3) and to a lesser extent by the accuracy of the CMM itself and the measuring strategy (see section 5).

Table 7. Summary of the Pareto Charts. Main effects and interactions in Ra, Ry, Rz, ε.

	Ti-6Al-4V alloys				*Cr-Co* alloys			
	Ra	**Rz**	**Ry**	**E**	**Ra**	**Rz**	**Ry**	**ε**
Main effects	**f_n** (p-value **0.000**)	**f_n** (p-value **0.000**)	**f_n** (p-value **0.000**)	a_p (p-value 0.186)	**f_n** (p-value **0.009**)	f_n (p-value 0.276)	**R** (p-value **0.026**)	V_c (p-value 0.154)
	R (p-value 0.103)	a_p (p-value 0.304)	**R** (p-value **0.001**)	V_c (p-value 0.561)	V_c (p-value 0.071)	V_c (p-value 0.507)	V_c (p-value 0.449)	a_p (p-value 0.434)
	V_c (p-value 0.291)	V_c (p-value 0.304)	V_c (p-value 0.103)	R (p-value 0.845)	a_p (p-value 0.586)	a_p (p-value 0.515)	f_n (p-value 0.481)	f_n (p-value 0.533)
	a_p (p-value 0.500)	R (p-value 0.796)	a_p (p-value 0.539)	f_n (p-value 0.922)	R (p-value 1.000)	R (p-value 0.755)	a_p (p-value 0.592)	R (p-value 0.989)
Interaction effects	**$V_c \times a_p$** (p-value **0.002**)	**$V_c \times a_p$** (p-value **0.000**)	**$V_c \times a_p$** (p-value **0.026**)	$V_c \times a_p$ (p-value 0.313)	$V_c \times a_p$ (p-value 0.053)	$V_c \times a_p$ (p-value 0.317)	$V_c \times a_p$ (p-value 0.189)	$V_c \times f_n$ (p-value 0.129)
	$V_c \times f_n$ (p-value 0.195)	**$V_c \times f_n$** (p-value **0.004**)	$V_c \times f_n$ (p-value 0.080)	$f_n \times a_p$ (p-value 0.424)	$f_n \times a_p$ (p-value 0.586)	$V_c \times f_n$ (p-value 0.355)	$V_c \times f_n$ (p-value 0.320)	$V_c \times a_p$ (p-value 0.182)
	$f_n \times a_p$ (p-value 0.683)	$f_n \times a_p$ (p-value 0.627)	$f_n \times a_p$ (p-value 0.782)	$V_c \times f_n$ (p-value 0.650)	$V_c \times f_n$ (p-value 0.855)	$f_n \times a_p$ (p-value 0.625)	$f_n \times a_p$ (p-value 0.716)	$f_n \times a_p$ (p-value 0.769)

[Insert Table 7]

In order to prove the results of the influence of the cutting parameters on part quality, a short testing DoE was conducted. This DoE checks the worst and best cutting combinations for surface roughness in both *Ti-6Al-4V* and *Cr-Co* alloys. According to the results shown above, for *Ti-6Al-4V* alloys the best cutting combination is V_c = 80 m/min, f_n = 0.05 mm and a_p = 0.1 mm whereas the worst combination is V_c = 80 m/min, f_n = 0.2 mm and a_p = 0.3 mm. Both cutting conditions are independent of the radius of curvature, so both experiments were conducted at R = 30 mm for simplicity. On the other hand, for *Cr-Co* alloys the best cutting combination is V_c = 35 m/min, f_n = 0.05 mm and a_p = 0.1 when turning features with radius of curvature of 10 mm, whereas the worst combination is V_c = 35 m/min, f_n = 0.15 mm and a_p = 0.1 mm when turning features with radius 30 mm. These four experiments were conducted to check the influence of cutting parameters in the specific application of spherical prostheses. Results shown in Table 8, confirm the influence on the average of all surface roughness parameters discussed above.

5.2.1 Comparison of machinability between Ti-6Al-4V and Cr-Co alloys

To show the differences in machinability when cutting *Ti-6Al-4V* or *Cr-Co* alloys, several ANOVA analyses were conducted to demonstrate the importance of the properties of prosthesis materials during machining, in terms of surface roughness parameters (*Ra*, *Ry* and *Rz*) and form deviation. The ANOVA analyses involving surface roughness parameters were conducted with the cutting data obtained when machining at f_n = 0.05 mm/rev and low or high levels of cutting depths, cutting speeds and radii of the spherical features in order to avoid the influence of the main effect f_n in the analysis. The ANOVA analysis of spherical form deviation was conducted with all cutting data, since no main effects or interactions were detected for this performance variable. The ANOVA results shown in Tables 9-13 and Figures 7-10 reveal details that would be of interest to manufactures of prostheses.

The ANOVA analysis presented in Table 9 shows that the surface roughness parameter *Ra* has an important bias between the two prosthesis materials. As it is shown in the boxplot in Figure 7, *Ti-6Al-4V* alloys present a lower *Ra* value at low feed rates than *Cr-Co* alloys (0.23 *μm* vs. 0.30 *μm*), which is an indicator of the better machinability of the former alloy in comparison with Cr-Co in the field of prostheses manufacturing. For the surface roughness parameters *Ry* and *Rz*, the ANOVA analyses presented in Tables 10 and 11 do not reveal a significant bias deviation related to the material used for the prosthesis. However, it seems that an important variability in *Ry* and *Rz* parameters does

show up when machining *Cr-Co* alloys, as shown in Figures 8 and 9. An F-test was conducted to analyse whether Ry and Rz present significant variability when machining these alloys. The hypothesis testing shown in Tables 12 and 13 confirm a higher variability of Ry and Rz parameters of *Cr-Co* alloys in comparison to *Ti-6Al-4V*. This fact could be explained by the higher stochastic effects of plastic deformation in *Cr-Co* alloys when machining at low feed rates, where the cutting operation transits from micro-cutting to ploughing [25]. Furthermore, the higher hardness of *Cr-Co* alloys may produce a rapid cutting-tool deterioration that can affect the surface quality even when the cutting-tool used at the beginning of the operation is new.

Table 9. Analysis of Variance for Surface Roughness (Ra)

Source	DF	SS	MS	F	p-value
Material	1	0.02403	0.02403	23.12	0.000
Error	14	0.01455	0.00104		
Total	15	0.03858			

[Insert Table 9]

Table 10. Analysis of Variance for Surface Roughness (Rz)

Source	DF	SS	MS	F	p-value
Material	1	0.494	0.494	4.52	0.052
Error	14	1.529	0.109		
Total	15	2.023			

[Insert Table 10]

Table 11. Analysis of Variance for Surface Roughness (Ry)

Source	DF	SS	MS	F	p-value
Material	1	0.446	0.446	2.48	0.138
Error	14	2.520	0.180		
Total	15	2.965			

[Insert Table 11]

Table 12. F-Test for equal variances for Rz

Material	Bonferroni confidence intervals for standard deviations		Standard Deviation
	Lower	Upper	
Ti-6Al-4V	0.1105	0.4046	0.1766
Cr-Co	0.2707	0.9911	0.4327

F-test	Test Statistic	0.167
	p-value	**0.031**

[Insert Table 12]

Table 13. F-Test for equal variances for Ry

Material	Bonferroni confidence intervals for standard deviations		Standard Deviation
	Lower	Upper	
Ti-6Al-4V	0.1033	0.3781	0.1651
Cr-Co	0.3608	1.3211	0.5768

F-test	Test Statistic	0.082
	p-value	**0.004**

[Insert Table 13]

Fig. 7 Boxplot of *Ra* according to workpiece material

Boxplots of Ra by material
(means are indicated by solid circles)
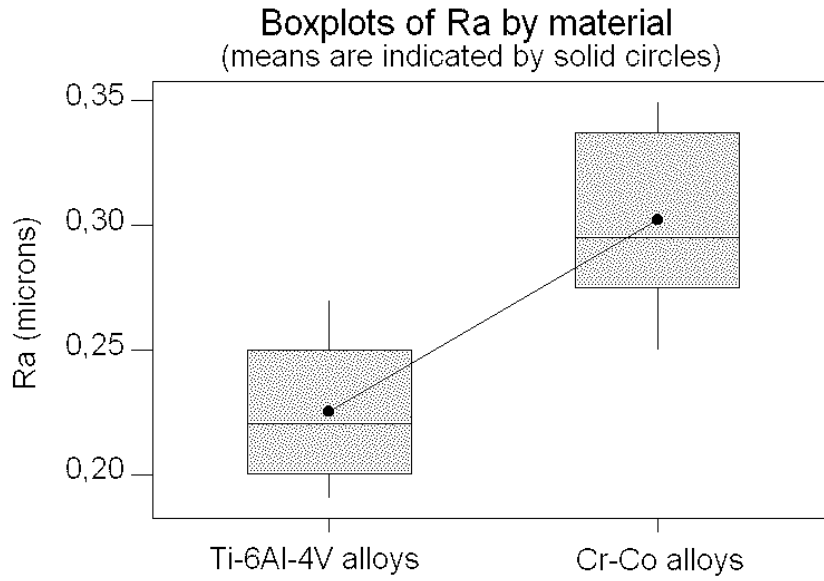
[Insert Figure 7]

Fig. 8. Boxplot of *Ry* according to workpiece material

Boxplots of Ry by material
(means are indicated by solid circles)
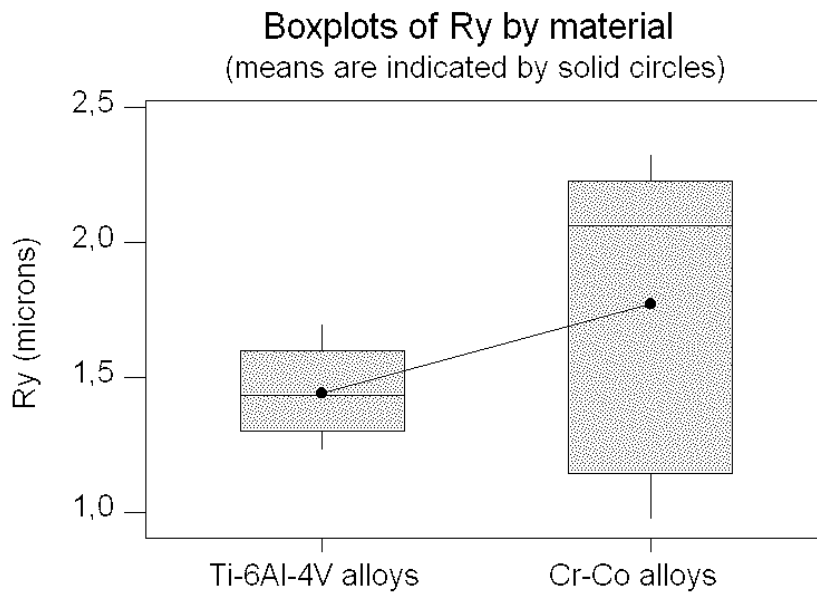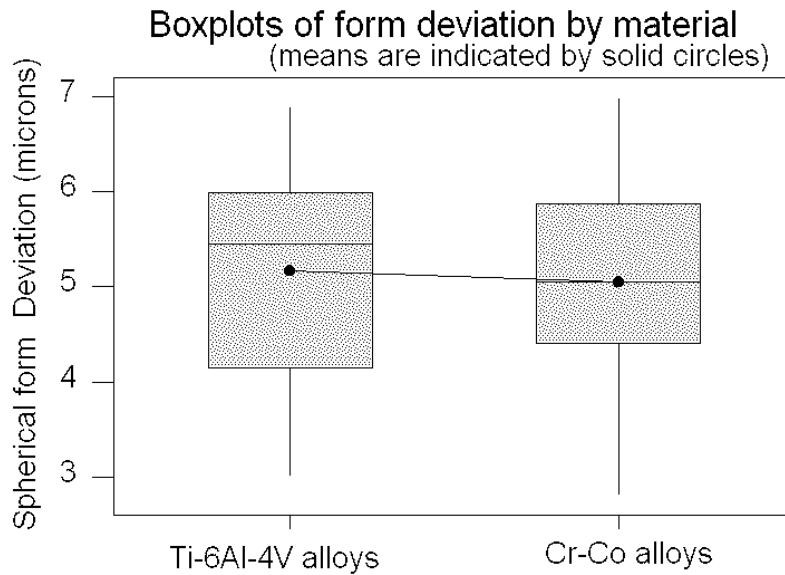
[Insert Figure 8]

Fig. 9. Boxplot of *Rz* according to workpiece material
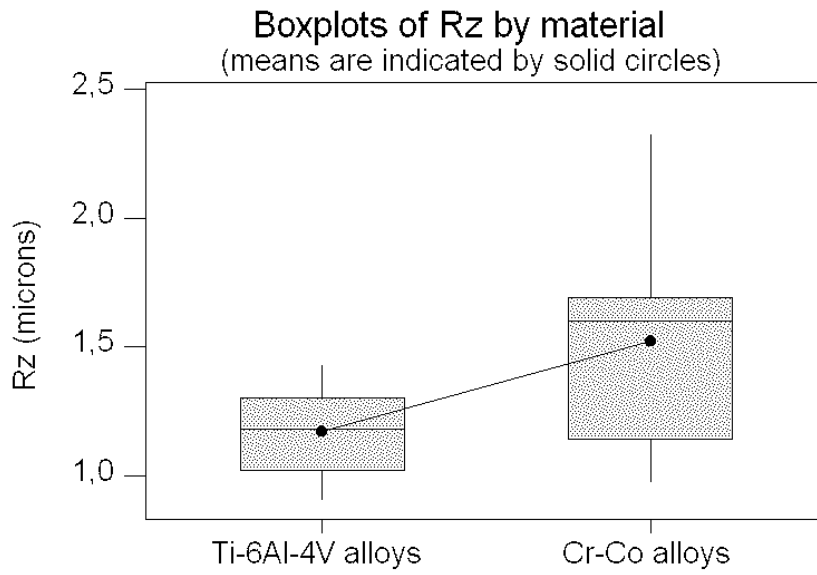
[Insert Figure 9]

Fig. 10. Boxplots of spherical form deviation *ε* according to workpiece material

[Insert Figure 10]

Finally, there are no differences in spherical form deviation between *Ti-6Al-4V* and *Cr-Co* alloys, as shown in the ANOVA analysis in Table 14 and the boxplot in Figure 10. This fact confirms the reasoning followed above, whereby the results of the Pareto diagrams indicated that form deviation may be mainly explained by the CNC lathe accuracy and the accuracy of the CMM measurements and the measuring strategy. This testing shows that the spherical form deviation in the manufacture of medium-size prostheses is not a critical issue when adequate equipment and cutting parameters are used, since spherical form deviation of 10 *μm* or lower is a commonly admissible deviation in spherical prosthesis manufacturing.

Table 14. Analysis of Variance for spherical form deviation ε

Source	DF	SS	MS	F	p-value
Material	1	0.3e-6	0.3e-6	0.12	0.736
Error	30	776e-7	2.6e-6		
Total	31	779e-7			

[Insert Table 14]

5.2.2 Machinability at low feed rates

The surface roughness and tight geometrical tolerances specified in prostheses manufacturing demand low feed rates in machining operations. But it is well known that the machinability of any workpiece material is poor when machining at very low feed rates (usually when *f_n<0.1 mm/rev*) due to the plastic deformation and other phenomena [25]. In this subsection, the machinability of both biocompatible materials at low feed rates is discussed, focusing the study on the surface roughness parameter *R_z*, a parameter close related to surface protection against corrosion [16].

According to cutting theory, the theoretical value of the surface roughness parameter *R_z* is usually determined from the well-known relation [26]:

$$R_{zt} = \frac{0.125 f_n{}^2}{r_e},$$

(1)

where *r_e* is the corner radius of the cutting-tool. However, when turning at low feed rates, the surface roughness is limited by the plastic deformation and its value is notably higher than that predicted by Eq. (1). An additional purely geometric term, which includes the

minimal removable chip thickness h_{min}, was proposed by Brammertz to take these effects into account. Brammertz's formula was defined as [27]:

$$R_{zt}^B = \frac{0.125 f_n{}^2}{r_e}$$
$$+ \frac{h_{min}}{2} \left(1 + \frac{r_e\, h_{min}}{f_n{}^2} \right),$$

(2)

where the minimal removable chip thickness h_{min} is related to the critical depth of penetration, which in turn corresponds to the transition from ploughing to micro-cutting [25]. Note that in Eq. (2) h_{min} should be expressed in *mm*, f_n in *mm/rev* and r_e in *mm*. The effect of plastic flow on turning/micro-turning has been analysed in different research studies [25, 28].

In order to analyse the plastic deformation at low feed rates and ensure minimum surface roughness in the manufacture of prostheses, an additional DoE was conducted (Table 15). For isolating the effects of low feed rates on cutting operations with the two biocompatible materials, the radius and cutting speed were fixed at a high level whereas the cutting depth was fixed at a low level.

Table 15. Additional DoE to analyse the effect of plastic deformation on surface roughness parameters

|	V_c (m/min)	f_n (mm/rev)	a_p (mm)	R (mm)	Ra (µm)	Rz (µm)	Ry (µm)
Ti-6Al-4V Alloys	80.00	0.05	0.10	30	0.20	0.90	1.50
	80.00	0.100	0.100	30	0.21	1.20	1.30
	80.00	0.125	0.100	30	0.24	1.23	1.53
	80.00	0.150	0.100	30	0.30	1.57	2.00
	80.00	0.200	0.100	30	0.34	1.83	2.20
	80.00	0.05	0.10	30	0.19	1.00	1.70
	80.00	0.100	0.100	30	0.26	1.40	1.60
	80.00	0.125	0.100	30	0.25	1.13	1.53
	80.00	0.150	0.100	30	0.26	1.47	1.70
	80.00	0.200	0.100	30	0.33	1.83	2.10
Cr-Co Alloys	35.00	0.05	0.10	30	0.30	1.67	2.13
	35.00	0.075	0.100	30	0.27	1.43	1.83
	35.00	0.100	0.100	30	0.34	1.63	2.27
	35.00	0.125	0.100	30	0.34	1.77	2.10
	35.00	0.150	0.100	30	0.38	1.93	2.33
	35.00	0.05	0.10	30	0.29	1.53	2.00
	35.00	0.075	0.100	30	0.23	1.23	1.43
	35.00	0.100	0.100	30	0.33	1.70	2.60
	35.00	0.125	0.100	30	0.30	1.63	2.30
	35.00	0.150	0.100	30	0.34	1.63	1.83

[Insert Table 15]

The experimental results obtained with both *Ti-6Al-4V* and *Cr-Co* alloys show higher R_z values than those predicted by Eq. (1) due to the effects of plastic deformation. Brammertz's formula, shown in Eq. (2), was used to adjust the experimental data in order to obtain the minimal removable chip thickness for each biocompatible material and the cutting-tool used in the experimentation. Regressions showed an average minimal removable chip thickness h_{min} of 0.8 *µm* and 1.3 *µm* for *Ti-6Al-4V* and *Cr-Co* alloys and correlation coefficients of $R^2 = 83.9\%$ and $R^2 = 35.9\%$ respectively. The high value of the coefficient R^2 for *Ti-6Al-4V* with respect to *Cr-Co* alloys is due to a more deterministic behaviour of *Ti-6Al-4V* at low feed rates whereas when turning Cr-Co, the high variability

in the plastic deformation process prevents to fit with the Brammertz's formula with an enough level of accuracy.

Figure 11 shows the biases between the experimental values of Rz and the expected ones, considering the cutting-tool geometry (Eq. (1)) and Brammertz's formula (Eq. (2)). As can be observed, Rz values of *Ti-6Al-4V* alloys at the same feed rate are significantly lower than those of *Cr-Co* alloys due to their smaller value of h_{min}.

Fig. 11. Experimental Rz values, and theoretical values of R_{zt} and R^B_{zt} for *Ti-6Al-4V* and *Cr-Co* alloys.
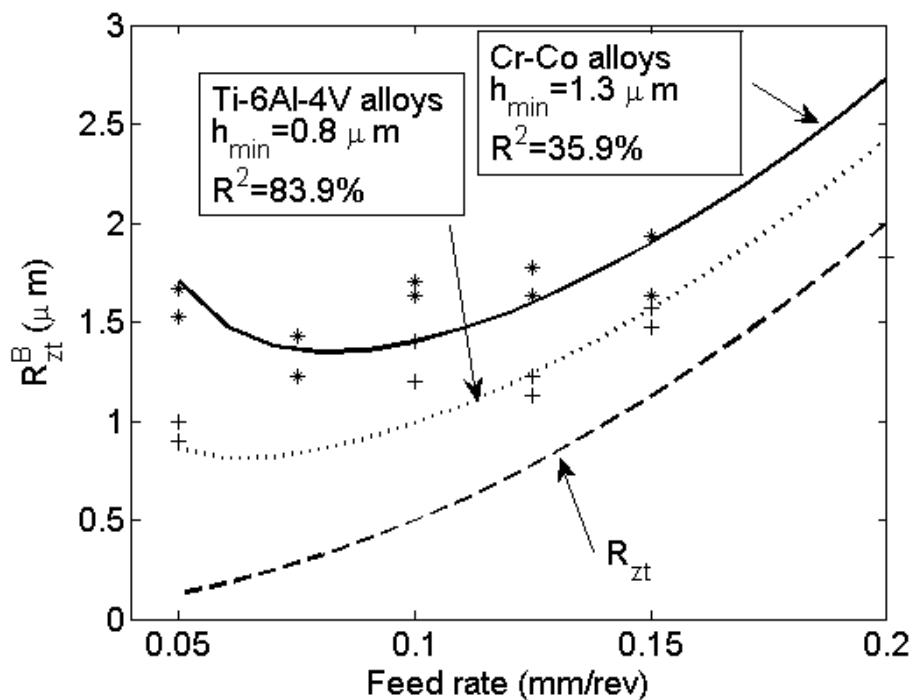
[Insert Figure 11]

6. Study of the influence of CMM parameters.

For the manufacture of spherical prostheses, due to the small size of the features to be measured, the intrinsic nature of the form tolerance to be evaluated (sphericity), and the high precision of the CMM (the repeatability of the CMM, which was evaluated according to the standard ASME B-89 1.12M, was measured as 1 *μm*), the most important source of error to be analysed is the measurement strategy. The sphericity error measured by a CMM is evaluated as the distance between the two concentric spheres that include all the measurement points whose centres are the same as the centre of the sphere that fits the measurement data through least squares [31]. According to this definition, the

26

deviations of the measurement points with respect to the sphere fitted by least squares can be assumed that follow a normal distribution. Thus, the sphericity error ε can be considered equal to *6s*, where *s* is the estimated standard deviation of the *n* measurement points with respect to the perfect sphere.

In order to evaluate the spherical form error, a measurement strategy should be defined. Some of the key aspects of the measurement strategy are: i) which points should be measured, how the centre point of the reference sphere will be evaluated, and how many points will be measured [30]. The first key aspect is defined according to the recommendations of the CMM manufacturer [32]. These recommendations suggest conducting the measurements in order to be uniformly distributed along the surface of the spherical feature. The first of the measurements should be placed on the top of the sphere, whereas the rest of the points should be equispaced and placed in different circular curves on the sphere. The second key aspect is defined by the algorithms used by the CMM. For the CMM used in the experimentation, as in most of the CMMs, the method to evaluate the centre point of the reference sphere is based on the least-squares centre [31].

Thus, for the manufacture of spherical prostheses, only the number of measurement points is defined as a parameter to be analysed which could influence on the result of the part quality inspected. In fact, the number of measurement points will define the range where the real value of the form error of the part lies for a given confidence interval. According to the number of points to be measured and assuming a normal distribution of the deviations of the measurement points with respect to the sphere fitted by least squares, the actual spherical form error will be laid within the range [γ_1, γ_2], where γ_1 and γ_2 depends on the number of measurement points and it is defined as [33]:

$$\gamma_1 = 6 \sqrt{\frac{(n-1)s^2}{\chi^2_{\frac{\alpha}{2},n-1}}}, \tag{3}$$

$$\gamma_2 = 6 \sqrt{\frac{(n-1)s^2}{\chi^2_{1-\frac{\alpha}{2},n-1}}}, \tag{4}$$

where *n* is the number of measurement points; *s* is estimated standard deviation of the *n* measurement points with respect to the perfect sphere fitted through least squares; α is referred to the confidence level of 100(1-α)% of the estimated range; and $\chi^2_{\frac{\alpha}{2},n-1}$ and $\chi^2_{1-\frac{\alpha}{2},n-1}$ are the lower and higher values corresponding to the α/2 percentage of a Chi

square distribution with *n-1* degrees of freedom, respectively. Thus, for a given measurement strategy, the actual spherical form error will lay within the range [γ_1, γ_2] with a confidence level of 100(1-α)%.

6.1 Design of Experiments.

In order to quantify the effect of the number of measurement points to assure the specifications of the prostheses, additional experimentation was conducted. For a given spherical part, the sphericity error was measured by four different number of measurement points: 5, 7, 9 and 17 measurement points. For each sphericity measurement, the range [γ_1, γ_2] where the actual sphericity error will lay with a confidence level of 95% was evaluated.

6.2 Analysis and discussion of the experimental results.

The results of the measurements are shown in Figure 12, where the measured value by the CMM and its range for a confidence level of 95% are drawn. As it can be seen, scattered measurements (5 and 7 points) estimate sphericity errors of 3.0 and 3.8 μm, inside the limits of 8.6 μm and 8.3 μm respectively with a confidence level of 95%. With 9 measurements, a good trade-off between the range where the actual error lies and the number of measurements is obtained. The 9 measurements estimates a sphericity error of 4.0 μm, and the actual sphericity error is assured to be lower than 7.6 μm with a confidence level of 95%. On the other hand, a high number of measurement points such as 17 points estimates a sphericity error of 4.3 μm, and assures that the actual sphericity error will be lower than 6.5 μm with a confidence level of 95%. However, for high number of measurements the time of inspection per part could be impractical. As a result, it can be noticed the importance of the number of measurement points to estimate the range where the actual sphericity error will lay with a confidence level of 95%. This range can be used to assure the sphericity tolerance of the spherical prosthesis.

Fig. 12. Influence of the number of measurement points in the estimation of the range with a confidence level of 95% where the actual value of the sphericity error of the part will lay.
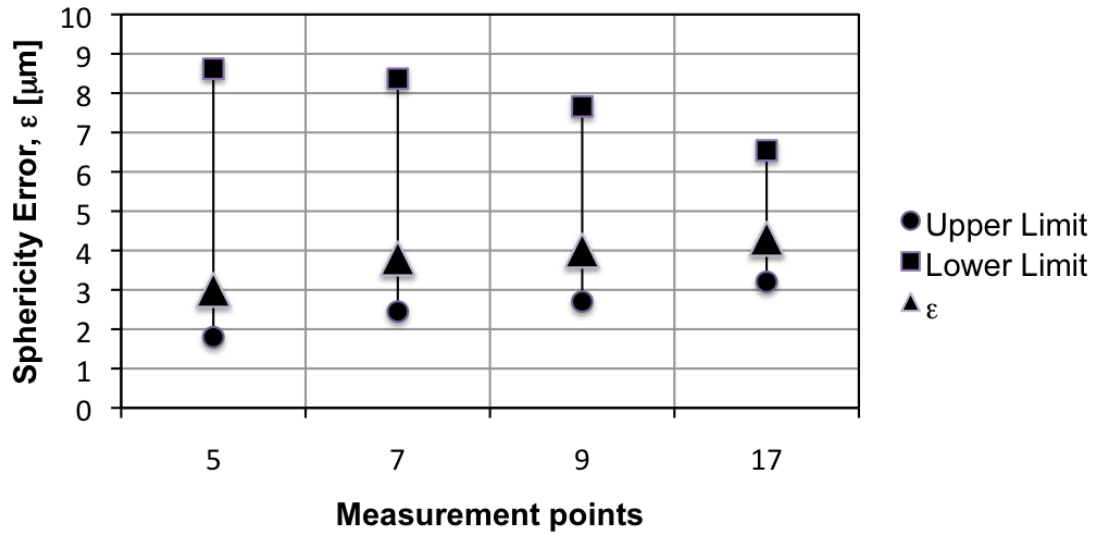
[Insert Figure 12]

7. Prediction of machining performance

7.1 Correlation of Sensor Measurements

In order to analyse the sensor information acquired by the experimentation, interaction effects plots of sensor measurements and factors were plotted for both *Ti-6Al-4V* and *Cr-Co* alloys, summarising their results in Table 16. In general, if machining is carried out under the cutting conditions recommended by the cutting-tool vendors, sensor signals are considerably higher in *Cr-Co* alloys than in *Ti-6Al-4V* alloys, which are mainly explained by the higher degree of hardness of *Cr-Co* alloys. In both cases, as shown in Table 16, all sensor signals are closely related to the main cutting parameter, that is, the feed rate f_n. The depth of cut also impacts all sensor signals except the vibrations on Z direction when turning Cr-Co alloys. However, the other process parameters, the cutting speed and the radius of the feature, only have a significant impact on a specific sensor signal. The cutting speed factor is not clearly related to any of the sensor signals acquired when turning *Ti-6Al-4V* alloys, although the cutting speed is closely related to both vibrations in the Z direction and acoustic emission signals when turning *Cr-Co* alloys. Interestingly, an increase in the cutting speed produces high levels of acoustic emission signals but also decreases the vibrations in the Z direction. According to Table 16, the radius of the feature machined is also important for the vibrations measurements Y and Z and the acoustic emission signals for both biocompatible materials, except for the vibrations on Z direction

when turning *Cr-Co* alloys. On the other hand, some interactions of the process variables have a significant impact on the sensor measurements. The interaction of feed rate and depth of cut is the most important interaction which impacts on all sensor signals except again the vibrations on Z direction when turning *Cr-Co* alloys. For *Ti-6Al-4V* alloys, the other interactions seem to be not significant except the interaction cutting speed and depth of cut for vibrations in Z direction. However, for *Cr-Co* alloys, all the interactions of the cutting parameters are relevant to the sensor measurements except for the vibrations in Z direction. This influence indicates a high sensitive of sensor signals to cutting parameters when turning *Cr-Co* alloys.

Table 16. Summary of the main effects and interactions of sensor measurements and process variables.

	Ti-6Al-4V alloys				*Cr-Co* alloys			
	RMS Acel X	RMS Acel Y	RMS Acel Z	RMS AE	RMS Acel X	RMS Acel Y	RMS Acel Z	RMS AE
Main effects	f_n (p-value 0.000)	f_n (p-value 0.001)	f_n (p-value 0.002)	f_n (p-value 0.000)	f_n (p-value 0.000)	f_n (p-value 0.000)	f_n (p-value 0.002)	f_n (p-value 0.000)
	a_p (p-value 0.001)	a_p (p-value 0.028)	R (p-value 0.012)	a_p (p-value 0.000)	a_p (p-value 0.000)	a_p (p-value 0.000)	V_c (p-value 0.022)	a_p (p-value 0.000)
	V_c (p-value 0.068)	R (p-value 0.042)	a_p (p-value 0.033)	R (p-value 0.029)	V_c (p-value 0.064)	R (p-value 0.001)	f_n (p-value 0.481)	V_c (p-value 0.000)
	R (p-value 0.205)	V_c (p-value 0.395)	V_c (p-value 0.518)	V_c (p-value 0.587)	R (p-value 0.334)	V_c (p-value 0.090)	a_p (p-value 0.273)	R (p-value 0.016)
Interaction effects	$f_n \times a_p$ (p-value 0.000)	$f_n \times a_p$ (p-value 0.006)	$f_n \times a_p$ (p-value 0.008)	$f_n \times a_p$ (p-value 0.000)	$V_c \times a_p$ (p-value 0.000)	$V_c \times a_p$ (p-value 0.002)	$V_c \times f_n$ (p-value 0.093)	$V_c \times f_n$ (p-value 0.000)
	$V_c \times f_n$ (p-value 0.160)	$V_c \times a_p$ (p-value 0.114)	$V_c \times a_p$ (p-value 0.048)	$V_c \times a_p$ (p-value 0.222)	$V_c \times f_n$ (p-value 0.002)	$V_c \times f_n$ (p-value 0.013)	$V_c \times a_p$ (p-value 0.227)	$V_c \times a_p$ (p-value 0.000)
	$V_c \times a_p$ (p-value 0.917)	$V_c \times f_n$ (p-value 0.629)	$V_c \times f_n$ (p-value 0.477)	$V_c \times f_n$ (p-value 0.882)	$f_n \times a_p$ (p-value 0.022)	$f_n \times a_p$ (p-value 0.037)	$f_n \times a_p$ (p-value 0.887)	$f_n \times a_p$ (p-value 0.003)

[Insert Table 16]

Table 17 summarizes the most important correlations between the machining performance variables *Ra, Ry, Rz* and *ε*, and the sensor signals used in this work. For *Ti-6Al-4V* alloys, the Table 17 shows that vibrations in the X direction are significant for the prediction of all surface roughness parameters, which can be explained mainly by the important influence that the feed rate has on X vibrations. Furthermore, the acoustic emission signal is correlated with both *Ra* and *Rz* values. This correlation could be explained by the high influence of the cutting depth on the acoustic emission, as shown

in Table 16. It is important to mention that no significant vibrations in Z and Y directions were observed in any performance variables.

Table 17. Summary of the correlation matrix between sensor measurements and machining performance variables.

		Ti-6Al-4V alloys			Cr-Co alloys			
	Ra	Ry	Rz	E	Ra	Ry	Rz	ε
	RMS X (p-value 0.005)	RMS X (p-value 0.022)	RMS X (p-value 0.006)	RMS X (p-value 0.779)	RMS Y (p-value 0.254)	RMS AE (p-value 0.206)	RMS AE (p-value 0.257)	RMS AE (p-value 0.001)
	RMS AE (p-value 0.028)	RMS AE (p-value 0.173)	RMS AE (p-value 0.018)	RMS Y (p-value 0.796)	RMS Z (p-value 0.260)	RMS Y (p-value 0.296)	RMS Y (p-value 0.475)	RMS Y (p-value 0.014)
	RMS Y (p-value 0.096)	RMS Y (p-value 0.341)	RMS Y (p-value 0.078)	RMS AE (p-value 0.831)	RMS AE (p-value 0.351)	RMS Z (p-value 0.662)	RMS Z (p-value 0.750)	RMS X (p-value 0.398)
Sensor Measurements	RMS Z (p-value 0.318)	RMS Z (p-value 0.598)	RMS Z (p-value 0.107)	RMS Z (p-value 0.891)	RMS X (p-value 0.467)	RMS X (p-value 0.865)	RMS X (p-value 0.892)	RMS Z (p-value 0.957)

[Insert Table 17]

Unlike *Ti-6Al-4V* alloys, for *Cr-Co* alloys the high variability in all surface roughness parameters prevents any correlation with any of the sensor measurements. However, statistically, the study shows that the spherical form deviation could be partially related to high levels of acoustic emission and vibrations in the Y direction. Although the experiment is short and the low levels of spherical form deviation are mostly due to the limited accuracy of the CNC lathe and the accuracy of CMM measurements, it seems that high vibration values and acoustic emission levels could reflect high cutting forces during cutting and, thus, possible cutting deflections and geometrical form errors. In fact, the vibrations in the Y direction are highly correlated with the cutting depth and the feed rate in *Cr-Co* alloys, and acoustic emission is highly correlated with cutting speed and feed rate. Hence, both sensor measurements could indirectly inform about the cutting forces and deflections in turning.

7.2 Reliability of the sensor system

The in-process sensor measurements were analysed to estimate the reliability of the use of these sensor signals to improve prediction of machining performance prediction within the range of the cutting conditions studied and, hence, to control product quality. To this end, several linear regressions were fitted with and without using the sensor information to predict the surface roughness parameters *Ra*, *Ry* and *Rz* and the spherical form

deviation ε. Tables 18 and 19 show the resulting regressions and their corresponding coefficient of determination R^2 and R^2_{adj} for *Ti-6Al-4V* and *Cr-Co* alloys.

An analysis of the R^2_{adj} coefficients (since they give a better estimation of the regression when few data is used) yielded several interesting results. In *Ti-6Al-4V* alloys, the cutting parameters are seen to account for 65.4%, 72.6% and 69.3% of the variability in the surface roughness parameters *Ra, Ry* and *Rz* respectively. Although these levels are rather low, the results can be considered acceptable since plastic deformation effects arise during turning due to the low feed rates that are applied. In order to predict spherical form deviation, a linear regression was fitted taking into account the cutting parameters that were applied. However, the random behaviour of this performance variable is confirmed by the lack of significance of each regression due to the accuracy limitations of the CNC lathe and the CMM measurements. Linear regressions for *Ra, Ry* and *Rz* were conducted with the addition of sensory information, but the results obtained did not improve the prediction to any notable extent. For *Ra* regressions, R^2_{adj} was increased to 67.9% by adding acoustic emission measurements and vibrations in the X direction.

Table 18. Linear regressions conducted in *Ti-6Al-4V* alloys

	Regressions of surface roughness parameters and form deviation
Without sensor information	$Ra = 0.142 + 0.967f_n + 2.86 \times 10^{-3}V_c \times a_p$ $R^2 = 70.0\%$; $R^2_{adj} = 65.4\%$
	$Ry = 0.645 + 4.18f_n + 0.0249\,R + 7.32 \times 10^{-3}V_c \times a_p$ $R^2 = 78.1\%$; $R^2_{adj} = 72.6\%$
	$Rz = 0.912 + 2.74f_n + 1.42 \times 10^{-2}V_c \times f_n + 6.58 \times 10^{-3}V_c \times a_p$ $R^2 = 75.5\%$; $R^2_{adj} = 69.3\%$
	$\varepsilon \rightarrow$ No significant regression
With sensor Information	$Ra = 0.145 + 1.01f_n + 2.31 \times 10^{-3}V_c \times a_p - 2.919 \times 10^{-5}RMS\,AE + 2.67 \times 10^{-4}RMS\,X$ $R^2 = 78.1\%$; $R^2_{adj} = 69.3\%$
	$Ry \rightarrow$ Sensors do not improve surface roughness prediction
	$Rz \rightarrow$ Sensors do not improve surface roughness prediction
	$\varepsilon \rightarrow$ No significant regression

[Insert Table 18]

Table 19. Linear regressions conducted in *Cr-Co* alloys

	Regressions of surface roughness parameters and form deviation
	$Ra = 0.314 + 0.450f_n - 1.37 \times 10^{-3}V_c$

Without sensor Information	$R^2 = 53.5\%$; $R^2_{adj} = 46.3\%$
	$Ry = 1.35 + 0.0245R$ $R^2 = 36.8\%$; $R^2_{adj} = 32.3\%$
	$Rz \rightarrow$ No significant regression
	$\varepsilon \rightarrow$ No significant regression
With sensor Information	$Ra = 0.289 + 0.627f_n + 1.06 \times 10^{-4}RMS\,Y - 8.48 \times 10^{-6}RMS\,AE - 4.7 \times 10^{-5}RMS\,X$ $R^2 = 61.4\%$; $R^2_{adj} = 47.4\%$
	$Ry \rightarrow$ Sensors do not improve surface roughness prediction
	$Rz = 1.56 + 4.78f_n - 7.99 \times 10^{-4}RMS\,X$ $R^2 = 32.6\%$; $R^2_{adj} = 22.3\%$
	$\varepsilon = 3.95 + 4.8 \times 10^{-5}RMS\,Y + 4.6 \times 10^{-4}RMS\,AE$ $R^2 = 55.0\%$; $R^2_{adj} = 48.1\%$

[Insert Table 19]

For *Cr-Co* alloys, the regression models fitted for the machining performance variables *Ra* and *Rz* were considerably less significant than those fitted for *Ti-6Al-4V* alloys. The low values of R^2_{adj} for *Cr-Co* alloys indicate a high degree of variability when turning these alloys at low feed rates and this, in turn, makes it impossible to ensure that tight surface roughness specifications are maintained. In fact, without adding sensory information, the surface roughness *Ra* and *Ry* was fitted with a R^2_{adj} of 46.3% and 32.3% respectively, but it was not possible to fit the *Rz* variable and the spherical form deviation with a significant linear regression. However, statistically, it seems that the sensor measurements report more information about the cutting process when turning *Cr-Co* alloys. By adding the sensor signals as predictor variables, the linear regressions for surface roughness *Ra*, *Rz* and form deviation increase the R^2_{adj} to 47.4%, 22.3% and 48.1% respectively, although there is no improvement when fitting the *Ry* parameter. Although these values are relatively low, they show that sensor information is complementary to cutting parameters and could slightly improve the resulting regressions.

However, in spite of the increase in the R^2_{adj} coefficient in both *Ti-6Al-4V* and *Cr-Co* alloys, their low rates reveal that the effects of plastic deformation generate an important degree of variability in machining performance, especially in *Cr-Co* alloys. This variability makes it impossible to use simple linear regressions with or without sensory information to reach reliable prediction systems with which to control the manufacturing

process accurately. Thus, in order to overcome the current limitations, more complex systems such as artificial neural networks (ANN) should be explored.

8. Conclusions

A study of the effects of process variables on part quality (surface roughness and sphericity tolerance) was conducted to compare the machining performance of *Ti-6Al-4V* and *Cr-Co* alloys in turning spherical prosthesis parts. Three independent analyses were conducted: a first analysis dealt with the influence of machine-tool and CNC parameters on the part quality of the spherical features; a second analysis dealt with the influence of machining parameters and curvature of the part on surface roughness parameters and spherical form deviation; and a third analysis dealt with the influence of the CMM parameters on the inspection of the sphericity error of the prostheses.

In the first analysis, the effect of the following errors during cutting-tool movements was considered as the most important factor on the contour error of the part. However, in spite of the following errors reported during the turning, the sphericity error which was the main characteristic to keep under control in the spherical prostheses was always kept lower than 9 μm. In the second analysis, the results showed that when turning *Ti-6Al-4V,* several cutting parameters, such as the feed rate and the interaction between cutting speed and depth of cut, are correlated with surface quality. However, in the case of *Cr-Co* alloys, only the feed rate seems to be slightly significant and all surface roughness parameters presented a high degree of variability. The results also showed that the spherical form deviation was not affected by any of the factors analysed, and its low value was mainly explained by the accuracy of the CNC lathe and the accuracy of the CMM measurements. A close comparison of both biocompatible materials revealed that the machining performance of *Ti-6Al-4V* alloys is higher than that of *Cr-Co* alloys, since the surface roughness parameters *Ra*, *Ry* and *Rz* are lower and have less variability. On the other hand, since a low and controlled surface roughness is required in the manufacture of prostheses, an additional study with more experimental data was conducted at low feed rates. Under these conditions, plastic deformation effects arise and determine the minimum surface roughness achievable, which depends on the minimal removable chip thickness h_{min}. According to the experimental results, *Ti-6Al-4V* alloys presented a lower h_{min} value than *Cr-Co,* which means lower values of surface roughness parameters.

In the third analysis, the influence of the CMM on the inspection of the sphericity error was basically explained through the number of measurement points measured to evaluate the sphericity characteristic. According to the number of points, the range where the actual value of the sphericity error of a part lies can be reduced up to a desired value to assure prosthesis specifications with a specific confidence level.

Finally, an additional study of the sensor measurements obtained from a low-cost non-intrusive multi-sensor system was conducted in order to investigate its potential use as a means of predicting machining performance. The results showed that the use of sensor measurements as regressors only slightly improves the surface roughness predictions in comparison to those conducted without sensor measurements, since most of the information given by the sensors is related to the cutting parameters. Only the sensor measurements of the acoustic emission sensor and the accelerometer in the X direction seem to add some complementary information from the cutting process. Furthermore, the low R^2_{adj} coefficients obtained for any regression in both biocompatible materials reveals that the plastic deformation effects generate an important amount of variability in machining performance, which prevents the use of any simple linear regression for a reliable prediction of machining performance. This is especially true in *Cr-Co* alloys, where the R^2_{adj} coefficients for all surface roughness parameters are lower than 50%, whereas for *Ti-6Al-4V* alloys they are around 70%. Thus, for this experimental study, the multi-sensor system does not provide higher prediction reliability and other complex models such as ANN models should be investigated to justify the investment in sensor systems for this specific application.

Acknowledgements

References

[1]   Balazic M, Kopac J, Jackson MJ, Ahmed W (2007) Review: titanium and titanium alloy applications in medicine. Int J Nano Biomater 1:3-34.

[2]   Long M, Rack HJ (1998) Titanium alloys in total joint replacement - a materials science perspective. Biomater 19: 1621-1639.

[3]   Ohkubo C, Watanabe I, Ford JP, Nakajima H, Hosoi T, Okabe T (2000) The machinability of cast titanium and Ti-6Al-4V, Biomater 21:421-428.

[4]   Yang X, Liu CR (1999) Machining Titanium and its Alloys. Mater Sci Technol 3:107-139.

[5]   Barry J, Byrne G, Lennon D (2001) Observations on chip formation and acoustic emission in machining Ti-6Al-4V alloy. Int J Mach Tools Manuf 41:1055-1070.

[6]   Ezugwu EO (2005) Key improvements in the machining of difficult-to-cut aerospace alloys, Int J Mach Tools Manuf 45:1353-1367.

[7]   Ezugwu EO, Da Silva RB, Bonney J, Machado AR (2005) Evaluation of the performance of CBN tools when turning Ti-6Al-4V. Int J Mach Tools Manuf 45:1009-1014.

[8]   Aspinwall DK, Dewes RC, Mantle AL (2005) The machining of gamma-TiAl Intermetallic Alloys. CIRP Ann 54:99-104.

[9]   López de Lacalle LN, Pérez-Bilbatua J, Sánchez JA, Llorente JI, Gutierrez A, Albóniga J (2000) Using High Pressure Coolant in the Drilling and Turning of Low Machinability Alloys. Int J Adv Manuf Technol 16:85-91.

[10]   Aydin AK (1991) Evaluation of finishing and polishing techniques on surface roughness of chromium-cobalt castings. J Prosthet Dent 65:763-767.

[11]   Xenodimitropoulou G, Radford DR (1998) The machining of cobalt-chromium alloy in partial denture. Int J Prosthodont, 11(6): 565-73.

[12]   Shi AJ (2008) Biomedical Manufacturing: A new Frontier of Manufacturing Research. J Manuf Sci Eng 130: 021009-1-021009-8.

[13]   Grill A (2003) Diamond-like carbon coatings as biocompatible materials - an overview. Diamond Relat Mater 12:166-170.

[14]   Camalaz M, Coupard D, Girot F (2008) A new material model for 2D numerical simulation of serrated chip formation when machining titanium alloy Ti–6Al–4V, Int J Mach Tools Manuf 48:275-288.

[15]   Gadelmawla ES, Koura MM, Maksoud TMA, Elewa IM, Soliman HH (2002) Roughness parameters. J Mater Process Technol 123:133-145.

[16]   Stephenson, D. A., Agapiou, J.S, Metal Cutting Theory and Practice, Marcel Dekker, New York, 1997.

[17]   Ramesh R, Mannan MA, Poo AN (2000) Error compensation in machine tools - a review. Part I: Geometric, cutting-force induced and fixture-dependent errors. Int J Mach Tools Manuf 40:1235-1256.

[18]   Ramesh R, Mannan MA, Poo AN (2000) Error compensation in machine tools - a review. Part II: Thermal errors, Int J Mach Tools Manuf 40:1257-1284.

[19]   Tikhon M, Ko TJ, Lee SH, Sool Kim H (2004) NURBS interpolator for constant material removal rate in open NC machine tools, Int J Mach Tools Manuf 44:237-245.

[20]   López de Lacalle LN, Lamikiz A (2009) Machine Tools for High Performance Machining. Springer London.

[21]   Ramesh R, Mannan MA, Poo AN (2005) Tracking and contour error control in CNC servo systems, Int J Mach Tools Manuf 45:301-326.

[22]   Liang M, Mgwatu M, Zuo M (2001) Integration of cutting parameter selection and tool adjustment decisions for multipass turning. Int J Adv Manuf Technol 17:861–869.

[23]   Feng CXJ, Wang X (2002) Development of empirical models for surface roughness prediction in finish turning. Int J Adv Manuf Technol 20:348–356.

[24]   Benardos PG, Vosniakos GC (2003) Predicting surface roughness in machining: A review. Int J Mach Tools Manuf 43:833-844.

[25]   Grzesik W (1996) A revised Model for predicting surface roughness in turning, Wear 194:143-148.

[26]   Boothroyd, G., Knight, W. A., Fundamentals of Machining and Machine Tools, Marcel Dekker, New York, 1989.

[27]   Brammertz, P. H., Die Entstehung der Oberflächenrauheit beim Feindrehem, Industrie Anzeiger, 2, (1961), 25-32.

[28]   Liu, K., Melkote, S. N., Effect of plastic side flow on surface roughness in micro-turning processes, International Journal of Machine Tools and Manufacture, 46 (2006) 1778-1785.

[29]   Schwenke H, Knapp W, Haitjema H, Weckenmann A, Schmitt R, Delbressine F (2008) Geometric error measurement and compensation of machines-An update
CIRP Ann 57:660-675.

[30]   Sun AYT, Anand S, Tang JSY (2002) Comprehensive design of experiments-based framework for optimal CMM inspection and uncertainty analysis of form tolerances. Intl J Prod Res 40: 2097 -2123.

[31]   Gass SI, Witzgall C, Harary HH (1998) Fitting circles and spheres to coordinate measuring machine data. Int J Flex Manuf Syst 10:5–25.

[32]   The Brown & Sharpe DEA MISTRAL Programming Manual (2000)

[33]   Montgomery D, Runger G (2007) Applied Statistics and Probability for engineers 4th Edition. John Wiley and Sons New Jersey 273-277.

Table Captions

Table 1. Experimental setup

Table 2. Measurement equipment for experimental work

Table 3. Sensors used in the experimentation

Table 4. Factors and levels analysed in the Design of Experiments

Table 5. Design of Experiments that was conducted and the resulting measurements of surface roughness and form deviation. Workpiece material: *Ti-6Al-4V* alloys

Table 6. Design of Experiments that was conducted and the resulting measurements of surface roughness and form deviation. Workpiece material: *Cr-Co* alloys

Table 7. Summary of the Pareto Charts. Main effects and interactions in *Ra, Ry, Rz, ε*

Table 8. Design of Experiments for testing the influence of cutting parameters on surface roughness and form deviation.

Table 9. Analysis of Variance for Surface Roughness (*Ra*)

Table 10. Analysis of Variance for Surface Roughness (*Rz*)

Table 11. Analysis of Variance for Surface Roughness (*Ry*)

Table 12. F-Test for equal variances for *Rz*

Table 13. F-Test for equal variances for *Ry*

Table 14. Analysis of Variance for spherical form deviation *ε*

Table 15. Additional DoE to analyse the effect of plastic deformation on surface roughness parameters

Table 16. Summary of the main effects and interactions of sensor measurements and process variables

Table 17. Summary of the correlation matrix between sensor measurements and machining performance variables

Table 18. Linear regressions conducted in *Ti-6Al-4V* alloys

Table 19. Linear regressions conducted in *Cr-Co* alloys

Figure Captions

Fig. 1 Manufacturing process plan for metallic components of prostheses.

Fig. 2 Experimental setup

Fig. 3 Machining operations carried out in the experimentation

Fig. 4 Equipment and Setup for off-line and in-process measurements

Fig. 5 Following errors of X and Z axis for different cutting combinations and radius of curvature.

Fig. 6 Sphericity error of the cutting-tool trajectory for different cutting combinations and radius of curvature.

Fig. 7 Boxplot of Ra according to workpiece material

Fig. 8. Boxplot of Ry according to workpiece material

Fig. 9. Boxplot of Rz according to workpiece material

Fig. 10. Boxplots of spherical form deviation ε according to workpiece material

Fig. 11. Experimental Rz values, and theoretical values of R_{zt} and R^B_{zt} for *Ti-6Al-4V* and *Cr-Co* alloys.

Fig. 12. Influence of the number of measurement points in the estimation of the range with a confidence level of 95% where the actual value of the sphericity error of the part will lay.